Chapter 11

The Electrooptic and Photorefractive Effects

11.1 Introduction to the Electrooptic Effect

The electrooptic effect is the change in refractive index of a material induced by the presence of a static (or low-frequency) electric field.

In some materials, the change in refractive index depends linearly on the strength of the applied electric field. This change is known as the linear electrooptic effect or Pockels effect. The linear electrooptic effect can be described in terms of a nonlinear polarization given by

$$P_i(\omega) = 2\epsilon_0 \sum_{jk} \chi^{(2)}_{ijk}(\omega = \omega + 0) E_j(\omega) E_k(0). \tag{11.1.1}$$

Since the linear electrooptic effect can be described by a second-order nonlinear susceptibility, it follows from the general discussion of Section 1.5 that a linear electrooptic effect can occur only for materials that are noncentrosymmetric. Although the linear electrooptic effect can be described in terms of a second-order nonlinear susceptibility, a very different mathematical formalism has historically been used to describe the electrooptic effect; this formalism is described in Section 11.2 of this chapter.

In centrosymmetric materials (such as liquids and glasses), the lowest-order change in the refractive index depends quadratically on the strength of the applied static (or low-frequency) field. This effect is known as the Kerr electrooptic effect* or as the quadratic electrooptic effect. It can be described in terms of a nonlinear polarization given by

$$P_i(\omega) = 3\epsilon_0 \sum_{jkl} \chi^{(3)}_{ijkl}(\omega = \omega + 0 + 0) E_j(\omega) E_k(0) E_l(0). \tag{11.1.2}$$

* The quadratic electrooptic effect is often referred to simply as the Kerr effect. More precisely, it is called the Kerr electrooptic effect to distinguish it from the Kerr magnetooptic effect.

Nonlinear Optics. https://doi.org/10.1016/B978-0-12-811002-7.00020-5

11.2 Linear Electrooptic Effect

In this section we develop a mathematical formalism that describes the linear electrooptic effect. Other treatments of the linear electrooptic effect are given in Cook and Jaffe (1979), Kaminow (1974), Thompson and Hartfield (1978), and Yariv and Yeh (1984). In an anisotropic material, the constitutive relation between the field vectors **D** and **E** has the form

$$D_i = \epsilon_0 \sum_j \epsilon_{ij} E_j \tag{11.2.1a}$$

or explicitly,

$$\begin{bmatrix} D_x \\ D_y \\ D_z \end{bmatrix} = \epsilon_0 \begin{bmatrix} \epsilon_{xx} & \epsilon_{xy} & \epsilon_{xz} \\ \epsilon_{yx} & \epsilon_{yy} & \epsilon_{yz} \\ \epsilon_{zx} & \epsilon_{zy} & \epsilon_{zz} \end{bmatrix} \begin{bmatrix} E_x \\ E_y \\ E_z \end{bmatrix}. \tag{11.2.1b}$$

For a lossless, non-optically active material, the dielectric permeability tensor ϵ_{ij} is represented by a real symmetric matrix, which therefore has six independent elements—that is, $\epsilon_{xx}, \epsilon_{yy}, \epsilon_{zz}, \epsilon_{xy} = \epsilon_{yx}, \epsilon_{xz} = \epsilon_{zx}$, and $\epsilon_{yz} = \epsilon_{zy}$. A general mathematical result states that any real, symmetric matrix can be expressed in diagonal form by means of an orthogonal transformation. Physically, this result implies that there exists some new coordinate system (X, Y, Z), related to the coordinate system x, y, z of Eq. (11.2.1b) by rotation of the coordinate axes, in which Eq. (11.2.1b) has the much simpler form

$$\begin{bmatrix} D_X \\ D_Y \\ D_Z \end{bmatrix} = \epsilon_0 \begin{bmatrix} \epsilon_{XX} & 0 & 0 \\ 0 & \epsilon_{YY} & 0 \\ 0 & 0 & \epsilon_{ZZ} \end{bmatrix} \begin{bmatrix} E_X \\ E_Y \\ E_Z \end{bmatrix}. \tag{11.2.2}$$

This new coordinate system is known as the principal-axis system, because in it the dielectric tensor is represented as a diagonal matrix.

We next consider the energy density per unit volume,

$$U = \tfrac{1}{2}\mathbf{D}\cdot\mathbf{E} = \tfrac{1}{2}\epsilon_0 \sum_{ij} \epsilon_{ij} E_i E_j, \tag{11.2.3}$$

associated with a wave propagating through the anisotropic medium. In the principal-axis coordinate system, the energy density can be expressed in terms of the components of the displacement vector as

$$U = \frac{1}{2\epsilon_0}\left[\frac{D_X^2}{\epsilon_{XX}} + \frac{D_Y^2}{\epsilon_{YY}} + \frac{D_Z^2}{\epsilon_{ZZ}}\right]. \tag{11.2.4}$$

This result shows that the surfaces of constant energy density in **D** space are ellipsoids. The shapes of these ellipsoids can be described in terms of the coordinates (X, Y, Z) themselves. If we let

$$X = \left(\frac{1}{2\epsilon_0 U}\right)^{1/2} D_X, \qquad Y = \left(\frac{1}{2\epsilon_0 U}\right)^{1/2} D_Y, \qquad Z = \left(\frac{1}{2\epsilon_0}\right)^{1/2} D_Z, \tag{11.2.5}$$

Eq. (11.2.4) becomes

$$\frac{X^2}{\epsilon_{XX}} + \frac{Y^2}{\epsilon_{YY}} + \frac{Z^2}{\epsilon_{ZZ}} = 1. \tag{11.2.6}$$

The surface described by this equation is known as the *optical indicatrix* or as the *index ellipsoid*. The equation describing the index ellipsoid takes on its simplest form in the principal-axis system; in other coordinate systems it is given by the general expression for an ellipsoid, which we write in the form

$$\left(\frac{1}{n^2}\right)_1 x^2 + \left(\frac{1}{n^2}\right)_2 y^2 + \left(\frac{1}{n^2}\right)_3 z^2 + 2\left(\frac{1}{n^2}\right)_4 yz + 2\left(\frac{1}{n^2}\right)_5 xz + 2\left(\frac{1}{n^2}\right)_6 xy = 1. \tag{11.2.7}$$

The coefficients $(1/n^2)_i$ are optical constants that describe the optical indicatrix in the new coordinate system; they can be expressed in terms of the coefficients $\epsilon_{XX}, \epsilon_{YY}, \epsilon_{ZZ}$ by means of the standard transformation laws for coordinate transformations, but the exact nature of the relationship is not needed for our present purposes.

The index ellipsoid can be used to describe the optical properties of an anisotropic material by means of the following procedure (Born and Wolf, 1975). For any given direction of propagation within the crystal, a plane perpendicular to the propagation vector and passing through the center of the ellipsoid is constructed. The curve formed by the intersection of this plane with the index ellipsoid forms an ellipse. The semimajor and semiminor axes of this ellipse give the two allowed values of the refractive index for this particular direction of propagation; the orientations of these axes give the polarization directions of the **D** vector associated with these refractive indices.

We next consider how the optical indicatrix is modified when the material system is subjected to a static or low-frequency electric field. This modification is conveniently described in terms of the *impermeability tensor* η_{ij}, which is defined by the relation

$$E_i = \frac{1}{\epsilon_0} \sum_j \eta_{ij} D_j. \tag{11.2.8}$$

Note that this relation is the inverse of that given by Eq. (11.2.1a), and thus that η_{ij} is the matrix inverse of ϵ_{ij}, that is, that $\eta_{ij} = (\epsilon^{-1})_{ij}$. We can express the optical indicatrix in terms of the elements of the impermeability tensor by noting that the energy density is equal to $U = (1/2\epsilon_0) \sum_{ij} \eta_{ij} D_i D_j$. If we now define coordinates x, y, z by means of relations $x = D_x/(2\epsilon_0 U)^{1/2}$, and so on, we find that the expression for U as a function of **D** becomes

$$1 = \eta_{11}x^2 + \eta_{22}y^2 + \eta_{33}z^2 + 2\eta_{12}xy + 2\eta_{23}yz + 2\eta_{13}xz. \tag{11.2.9}$$

By comparison of this expression for the optical indicatrix with that given by Eq. (11.2.7), we find that

$$\left(\frac{1}{n^2}\right)_1 = \eta_{11}, \qquad \left(\frac{1}{n^2}\right)_2 = \eta_{22}, \qquad \left(\frac{1}{n^2}\right)_3 = \eta_{33},$$
$$\left(\frac{1}{n^2}\right)_4 = \eta_{23} = \eta_{32}, \qquad \left(\frac{1}{n^2}\right)_5 = \eta_{13} = \eta_{31}, \qquad \left(\frac{1}{n^2}\right)_6 = \eta_{12} = \eta_{21}. \tag{11.2.10}$$

We next assume that η_{ij} can be expressed as a power series in the strength of the components E_k of the applied electric field as

$$\eta_{ij} = \eta_{ij}^{(0)} + \sum_k r_{ijk} E_k + \sum_{kl} s_{ijkl} E_k E_l + \cdots . \tag{11.2.11}$$

Here r_{ijk} is the tensor that describes the linear electrooptic effect, s_{ijkl} is the tensor that describes the quadratic electrooptic effect, etc. Since the dielectric permeability tensor ϵ_{ij} is real and symmetric, its inverse η_{ij} must also be real and symmetric, and consequently the electrooptic tensor r_{ijk} must be symmetric in its first two indices. For this reason, it is often convenient to represent the third-rank tensor r_{ijk} as a two-dimensional matrix r_{hk} using contracted notation according to the prescription

$$h = \begin{cases} 1 & \text{for } ij = 11, \\ 2 & \text{for } ij = 22, \\ 3 & \text{for } ij = 33, \\ 4 & \text{for } ij = 23 \text{ or } 32, \\ 5 & \text{for } ij = 13 \text{ or } 31, \\ 6 & \text{for } ij = 12 \text{ or } 21. \end{cases} \tag{11.2.12}$$

In terms of this contracted notation, we can express the lowest-order modification of the optical constants $(1/n^2)_i$ that appears in expression (11.2.7) for the optical indicatrix as

$$\Delta\left(\frac{1}{n^2}\right)_i = \sum_j r_{ij} E_j, \tag{11.2.13a}$$

where we have made use of Eqs. (11.2.10) and (11.2.11). This relationship can be written explicitly as

$$\begin{bmatrix} \Delta(1/n^2)_1 \\ \Delta(1/n^2)_2 \\ \Delta(1/n^2)_3 \\ \Delta(1/n^2)_4 \\ \Delta(1/n^2)_5 \\ \Delta(1/n^2)_6 \end{bmatrix} = \begin{bmatrix} r_{11} & r_{12} & r_{13} \\ r_{21} & r_{22} & r_{23} \\ r_{31} & r_{32} & r_{33} \\ r_{41} & r_{42} & r_{43} \\ r_{51} & r_{52} & r_{53} \\ r_{61} & r_{62} & r_{63} \end{bmatrix} \begin{bmatrix} E_x \\ E_y \\ E_z \end{bmatrix}. \tag{11.2.13b}$$

The quantities r_{ij} are known as the electrooptic coefficients and give the rate at which the coefficients $(1/n^2)_i$ change with increasing electric field strength.

We remarked earlier that the linear electrooptic effect vanishes for materials possessing inversion symmetry. Even for materials lacking inversion symmetry, where the coefficients do not necessarily vanish, the form of r_{ij} is restricted by any rotational symmetry properties that the material may possess. For example, for any material (such as ADP and potassium dihydrogen phosphate [KDP]) possessing the point group symmetry $\bar{4}2m$, the electrooptic coefficients must be of the form

$$r_{ij} = \begin{bmatrix} 0 & 0 & 0 \\ 0 & 0 & 0 \\ 0 & 0 & 0 \\ r_{41} & 0 & 0 \\ 0 & r_{41} & 0 \\ 0 & 0 & r_{63} \end{bmatrix} \quad \text{(for class } \bar{4}2m\text{)}, \tag{11.2.14}$$

where we have expressed r_{ij} in the standard crystallographic coordinate system, in which the Z direction represents the optic axis of the crystal. We see from Eq. (11.2.14) that the form of the symmetry properties of the point group $\bar{4}2m$ requires 15 of the electrooptic coefficients to vanish and two of the remaining coefficients to be equal. Hence, r_{ij} possesses only two independent elements in this case.

Similarly, the electrooptic coefficients of crystals of class $3m$ (such as lithium niobate) must be of the form

$$r_{ij} = \begin{bmatrix} 0 & -r_{22} & r_{13} \\ 0 & r_{22} & r_{13} \\ 0 & 0 & r_{33} \\ 0 & r_{42} & 0 \\ r_{42} & 0 & 0 \\ r_{22} & 0 & 0 \end{bmatrix} \quad \text{(for class } 3m\text{)}, \tag{11.2.15}$$

and the electrooptic coefficients of crystals of the class $4mm$ (such as barium titanate) must be of the form

$$r_{ij} = \begin{bmatrix} 0 & 0 & r_{13} \\ 0 & 0 & r_{13} \\ 0 & 0 & r_{33} \\ 0 & r_{42} & 0 \\ r_{42} & 0 & 0 \\ 0 & 0 & 0 \end{bmatrix} \quad \text{(for class } 4mm\text{)}. \tag{11.2.16}$$

The properties of several electrooptic materials are summarized in Table 11.2.1.

TABLE 11.2.1: Properties of several electrooptic materials[a].

Material	Point group	Electrooptic coefficients (10^{-12} m/V)	Refractive index
Potassium dihydrogen phosphate, KH_2PO_4 (KDP)	$\bar{4}2m$	$r_{41} = 8.77$ $r_{63} = 10.5$	$n_0 = 1.514$ $n_e = 1.472$ (at 0.5461 μm)
Potassium dideuterium phosphate, KD_2PO_4 (KD*P)	$\bar{4}2m$	$r_{41} = 8.8$ $r_{63} = 26.4$	$n_0 = 1.508$ $n_e = 1.468$ (at 0.5461 μm)
Lithium niobate, $LiNbO_3$	$3m$	$r_{13} = 9.6$ $r_{22} = 6.8$ $r_{33} = 30.9$ $r_{42} = 32.6$	$n_0 = 2.3410$ $n_e = 2.2457$ (at 0.5 μm)
Lithium tantalate, $LiTaO_3$	$3m$	$r_{13} = 8.4$ $r_{22} = -0.2$ $r_{33} = 30.5$ $r_{51} = 20$	$n_0 = 2.176$ $n_e = 2.180$ (at 0.633 nm)
Barium titanate, $BaTiO_3$[b]	$4mm$	$r_{13} = 19.5$ $r_{33} = 97$ $r_{42} = 1640$	$n_0 = 2.488$ $n_e = 2.424$ (at 514 nm)
Strontium barium niobate, $Sr_{0.6}Ba_{0.4}NbO_6$ (SBN:60)	$4mm$	$r_{13} = 55$ $r_{33} = 224$ $r_{42} = 80$	$n_0 = 2.367$ $n_e = 2.337$ (at 514 nm)
Zinc telluride, ZnTe	$\bar{4}3m$	$r_{41} = 4.0$	$n_0 = 2.99$ (at 0.633 μm)

[a] From a variety of sources. See, for example, B.J. Thompson and E. Hartfield in *The Handbook of Optics* (W.G. Driscoll and W. Vaughan, eds.), McGraw-Hill, New York, 1978, and W.R. Cook, Jr. and H. Jaffe, "Electrooptic Coefficients," in *Landolt-Bornstein, New Series*, Vol. II (K.-H. Hellwege, ed.), Springer-Verlag, 1979, pp. 552–651. The electrooptic coefficients are given in the MKS units of m/V. To convert to the cgs units of cm/statvolt each entry should be multiplied by 3×10^4.

[b] $\epsilon_{dc}^{\parallel} = 135, \epsilon_{dc}^{\perp} = 3700$.

11.3 Electrooptic Modulators

As an example of the application of the formalism developed in the last section, we now consider how to construct an electrooptic modulator using the material KDP. Of course, the analysis is formally identical for any electrooptic material of point group $\bar{4}2m$.

KDP is a uniaxial crystal, and hence in the absence of an applied electric field the index ellipsoid is given in the standard crystallographic coordinate system by the equation

$$\frac{X^2}{n_0^2} + \frac{Y^2}{n_0^2} + \frac{Z^2}{n_e^2} = 1. \tag{11.3.1}$$

Note that this (X, Y, Z) coordinate system is the principal-axis coordinate system in the absence of an applied electric field. If an electric field is applied to crystal, the index ellipsoid becomes modified according to Eqs. (11.2.13b) and (11.2.14) and takes the form

$$\frac{X^2}{n_0^2} + \frac{Y^2}{n_0^2} + \frac{Z^2}{n_e^2} + 2r_{41}E_X YZ + 2r_{41}E_Y XZ + 2r_{63}E_Z XY = 1. \tag{11.3.2}$$

Note that (since cross terms containing YZ, XZ, and XY appear in this equation) the (X, Y, Z) coordinate system is not the principal-axis coordinate system when an electric field is applied to the crystal. Note also that the crystal will no longer necessarily be uniaxial in the presence of a dc electric field.

Let us now assume that the applied electric field has only a Z component, so that Eq. (11.3.2) reduces to

$$\frac{X^2}{n_0^2} + \frac{Y^2}{n_0^2} + \frac{Z^2}{n_e^2} + 2r_{63}E_Z XY = 1. \tag{11.3.3}$$

This special case is often encountered in device applications. The new principal-axis coordinate system, which we designate (x, y, z), can now be found by inspection. If we let

$$X = \frac{x - y}{\sqrt{2}}, \qquad Y = \frac{x + y}{\sqrt{2}}, \qquad Z = z, \tag{11.3.4}$$

we find that Eq. (11.3.3) becomes

$$\left(\frac{1}{n_0^2} + r_{63}E_z\right)x^2 + \left(\frac{1}{n_0^2} - r_{63}E_z\right)y^2 + \frac{z^2}{n_e^2} = 1, \tag{11.3.5}$$

which describes an ellipsoid in its principal-axis system. This ellipsoid can alternatively be written as

$$\frac{x^2}{n_x^2} + \frac{y^2}{n_y^2} + \frac{z^2}{n_e^2} = 1, \tag{11.3.6}$$

where, in the physically realistic limit $r_{63}E_z \ll 1$, the new principal values of the refractive index are given by

$$n_x = n_0 - \tfrac{1}{2}n_0^3 r_{63}E_z, \tag{11.3.7a}$$

$$n_y = n_0 + \tfrac{1}{2}n_0^3 r_{63}E_z. \tag{11.3.7b}$$

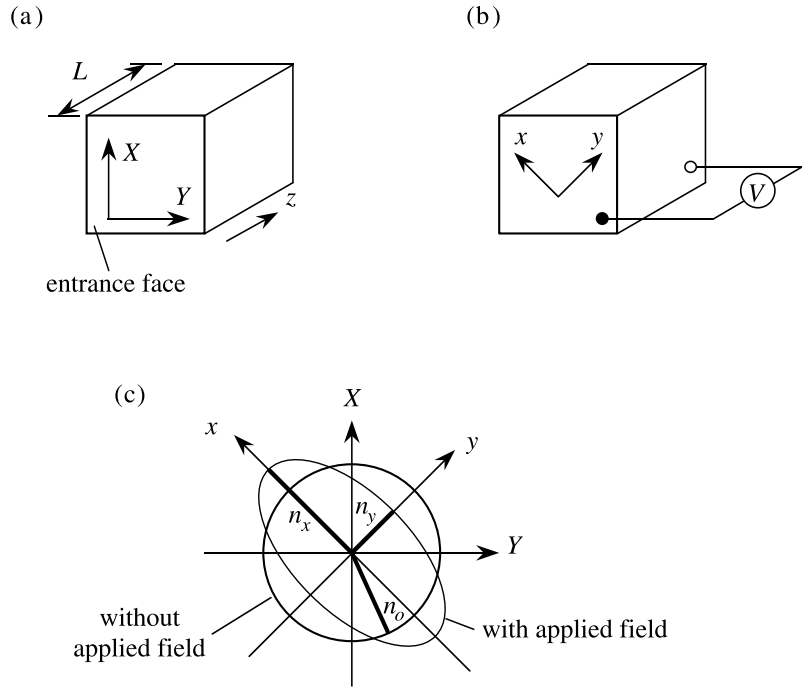

FIGURE 11.3.1: The electrooptic effect in KDP. (a) Principal axes in the absence of an applied field. (b) Principal axes in the presence of an applied field. (c) The intersection of the index ellipsoid with the plane $z = Z = 0$.

Fig. 11.3.1 shows how to construct a modulator based on the electrooptic effect in KDP. Part (a) shows a crystal that has been cut so that the optic axis (Z axis) is perpendicular to the plane of the entrance face, which contains the X and Y crystalline axes. Part (b) of the figure shows the same crystal in the presence of a longitudinal (z-directed) electric field $E_z = V/L$, which is established by applying a voltage V between the front and rear faces. The principal axes (x, y, z) of the index ellipsoid in the presence of this field are also indicated. In practice, the potential difference is applied by coating the front and rear faces with a thin film of a conductive coating. Historically, thin layers of gold have been used, although more recently the transparent conducting material indium tin oxide has successfully been used.

Part (c) of Fig. 11.3.1 shows the curve formed by the intersection of the plane perpendicular to the direction of propagation (i.e., the plane $z = Z = 0$) with the index ellipsoid. For the case in which no static field is applied, the curve has the form of a circle, showing that the refractive index has the value n_0 for any direction of polarization.* For the case in which a field is applied,

* The absence of birefringence effects in this situation is one of the primary motivations for orienting the crystal for propagation along the z direction.

this curve has the form of an ellipse. In drawing the figure, we have arbitrarily assumed that the factor $r_{63}E_z$ is negative; consequently the semimajor and semiminor axes of this ellipse are along the x and y directions and have lengths n_x and $n_y < n_x$, respectively.

Let us next consider a beam of light propagating in the $z = Z$ direction through the modulator crystal shown in Fig. 11.3.1. A wave polarized in the x direction propagates with a different phase velocity than a wave polarized in the y direction. In propagating through the length L of the modulator crystal, the x and y polarization components will thus acquire the phase difference

$$\Gamma = (n_y - n_x)\frac{\omega L}{c}, \tag{11.3.8}$$

which is known as the retardation. By introducing Eqs. (11.3.7) into this expression we find that

$$\Gamma = \frac{n_0^3 r_{63} E_z \omega L}{c}.$$

Since $E_z = V/L$, this result shows that the retardation introduced by a longitudinal electrooptic modulator depends only on the voltage V applied to the modulator and is independent of the length of the modulator. In particular, the retardation can be represented as

$$\Gamma = \frac{n_0^3 r_{63} \omega V}{c}. \tag{11.3.9}$$

It is convenient to express this result in terms of the quantity

$$V_{\lambda/2} = \frac{\pi c}{\omega n_0^3 r_{63}}, \tag{11.3.10}$$

which is known as the half-wave voltage. Eq. (11.3.9) then becomes

$$\Gamma = \pi \frac{V}{V_{\lambda/2}}. \tag{11.3.11}$$

Note that a half-wave (π radians) of retardation is introduced when the applied voltage is equal to the half-wave voltage. Half-wave voltages of longitudinal-field electrooptic materials are typically of the order of 10 kV for visible light.

Since the x and y polarization components of a beam of light generally experience different phase shifts in propagating through an electrooptic crystal, the state of polarization of the light leaving the modulator will generally be different from that of the incident light. Fig. 11.3.2 shows how the state of polarization of the light leaving the modular depends on the value of the retardation Γ for the case in which vertically (X) polarized light is incident on the modulator. Note that light of any ellipticity can be produced by controlling the voltage V applied to the modulator.

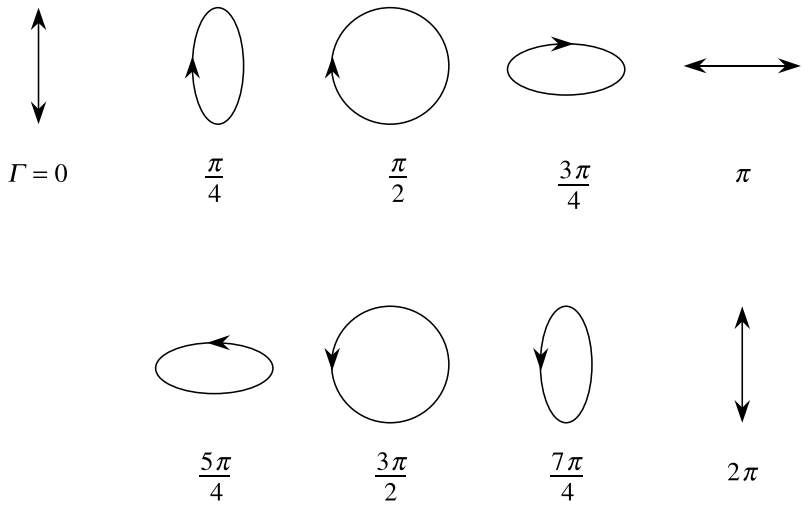

FIGURE 11.3.2: Polarization ellipses describing the light leaving the modulator of Fig. 11.3.1 for various values of the retardation. In all cases, the input light is linearly polarized in the vertical (X) direction.

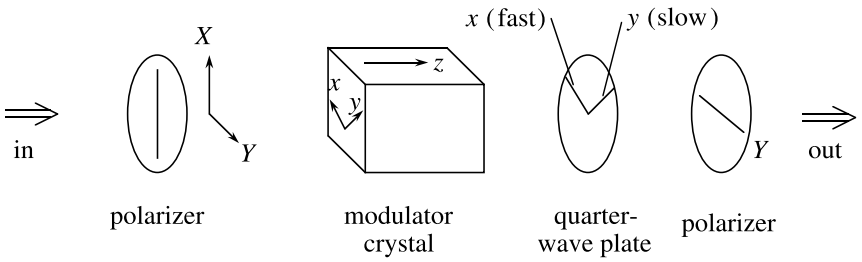

FIGURE 11.3.3: Construction of a voltage-controllable intensity modulator.

Fig. 11.3.3 shows one way of constructing an intensity modulator based on the configuration shown in Fig. 11.3.1. The incident light is passed through a linear polarizer whose transmission axis is oriented in the X direction. The light then enters the modulator crystal, where its x and y polarization components propagate with different velocities and acquire a phase difference, whose value is given by Eq. (11.3.11). The light leaving the modulator then passes through a quarter-wave plate oriented so that its fast and slow axes coincide with the x and y axes of the modulator crystal, respectively. The beam of light thereby acquires the additional retardation $\Gamma_B = \pi/2$. For reasons that will become apparent later, Γ_B is called the bias retardation. The total retardation is then given by

$$\Gamma = \pi \frac{V}{V_{\lambda/2}} + \frac{\pi}{2}. \tag{11.3.12}$$

In order to analyze the operation of this modulator, let us represent the electric field of the incident radiation after passing through the initial polarizer as

$$\tilde{\mathbf{E}} = \mathbf{E}_{\text{in}} e^{-i\omega t} + \text{c.c.}, \tag{11.3.13a}$$

where

$$\mathbf{E}_{\text{in}} = E_{\text{in}} \hat{\mathbf{X}} = \frac{E_{\text{in}}}{\sqrt{2}} (\hat{\mathbf{x}} + \hat{\mathbf{y}}). \tag{11.3.13b}$$

After the beam passes through the modulator crystal and quarter-wave plate, the phase of the y polarization component will be shifted with respect to that of the x polarization component by an amount Γ, so that (to within an unimportant overall phase factor) the complex field amplitude becomes

$$\mathbf{E} = \frac{E_{\text{in}}}{\sqrt{2}} \left(\hat{\mathbf{x}} + e^{i\Gamma} \hat{\mathbf{y}} \right). \tag{11.3.14}$$

Only the $\hat{\mathbf{Y}} = (-\hat{\mathbf{x}} + \hat{\mathbf{y}})/\sqrt{2}$ component of this field will be transmitted by the final polarizer. The field amplitude measured after this polarizer is hence given by $\mathbf{E}_{\text{out}} = (\mathbf{E} \cdot \hat{\mathbf{Y}})\hat{\mathbf{Y}}$, or by

$$\mathbf{E}_{\text{out}} = \frac{E_{\text{in}}}{2} \left(-1 + e^{i\Gamma} \right) \hat{\mathbf{Y}}. \tag{11.3.15}$$

If we now define the transmission T of the modulator of Fig. 11.3.3 as

$$T = \frac{|\mathbf{E}_{\text{out}}|^2}{|\mathbf{E}_{\text{in}}|^2}, \tag{11.3.16}$$

we find through use of Eq. (11.3.15) that the transmission is given by

$$T = \sin^2(\Gamma/2). \tag{11.3.17}$$

The functional form of these transfer characteristics is shown in Fig. 11.3.4. We see that the transmission can be made to vary from zero to one by varying the total retardation between zero and π radians. We can also see the motivation for inserting the quarter-wave plate into the setup of Fig. 11.3.3 in order to establish the bias retardation $\Gamma_B = \pi/2$. For the case in which the applied voltage V vanishes, the total retardation will be equal to the bias retardation, and the transmission of the modulator will be 50%. Since the transmission T varies approximately linearly with the retardation Γ for retardations near $\Gamma = \pi/2$, the transmission will vary nearly linearly with the value V of the applied voltage. For example, if the applied voltage is given by

$$V(t) = V_m \sin \omega_m t, \tag{11.3.18}$$

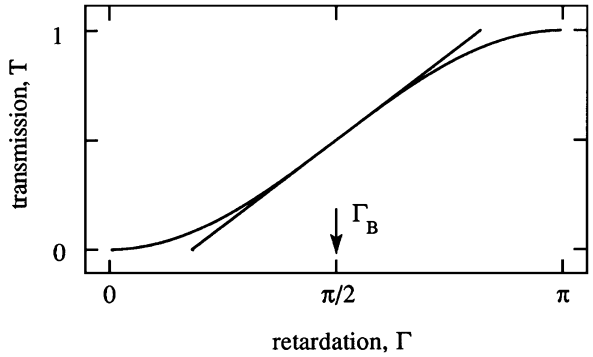

FIGURE 11.3.4: Transmission characteristics of the electrooptic modulator shown in Fig. 11.3.3.

the retardation will be given by

$$\Gamma = \frac{\pi}{2} + \frac{\pi V_m}{V_{\lambda/2}} \sin \omega_m t. \tag{11.3.19}$$

The transmission predicted by Eq. (11.3.17) is hence given by

$$T = \sin^2\left(\frac{\pi}{4} + \frac{\pi V_m}{2V_{\lambda/2}} \sin \omega_m t\right) \tag{11.3.20}$$

$$= \frac{1}{2}\left[1 + \sin\left(\frac{\pi V_m}{V_{\lambda/2}} \sin \omega_m t\right)\right], \tag{11.3.21}$$

which, for $\pi V_m / V_{\lambda/2} \ll 1$, becomes

$$T = \frac{1}{2}\left(1 + \frac{\pi V_m}{V_{\lambda/2}} \sin \omega_m t\right). \tag{11.3.22}$$

The electrooptic effect can also be used to construct a phase modulator for light. For example, if the light incident on the electrooptic crystal of Fig. 11.3.1 is linearly polarized along the x (or the y) axis of the crystal, the light will propagate with its state of polarization unchanged but with its phase shifted by an amount that depends on the value of the applied voltage. The voltage-dependent part of the phase shift is hence given by

$$\phi = (n_x - n_0)\frac{\omega L}{c} = -\frac{n_0^3 r_{63} E_z \omega L}{2c} = \frac{n_0^3 r_{63} V \omega}{2c}. \tag{11.3.23}$$

11.4 Introduction to the Photorefractive Effect

The photorefractive effect* is the change in refractive index of an optical material that results from the optically induced redistribution of electrons and holes. The photorefractive effect is quite different from most of the other nonlinear-optical effects described in this book in that it cannot be described by a nonlinear susceptibility $\chi^{(n)}$ for any value of n. The reason for this behavior is that, under a wide range of conditions, the change in refractive index in steady state is independent of the intensity of the light that induces the change. Because the photorefractive effect cannot be described by means of a nonlinear susceptibility, special methods must be employed to describe it; these methods are described in the next several sections. The photorefractive effect tends to give rise to a strong optical nonlinearity; experiments are routinely performed using milliwatts of laser power. However, the effect tends to be rather slow, with response times of 0.1 sec being typical.

The origin of the photorefractive effect is illustrated schematically in Fig. 11.4.1. We imagine that a photorefractive crystal is illuminated by two intersecting beams of light of the same frequency. These beams interfere to produce the spatially modulated intensity distribution $I(x)$ shown in the upper graph. Free charge carriers, which we assume to be electrons, are generated through photoionization at a rate that is proportional to the local value of the optical intensity.

These carriers can diffuse through the crystal or can drift in response to a static electric field. Both processes are observed experimentally. In drawing the figure we have assumed that diffusion is the dominant process, in which case the electron density is smallest in the regions of maximum optical intensity, because electrons have preferentially diffused away from these regions. The spatially varying charge distribution $\rho(x)$ gives rise to a spatially varying electric field distribution, whose form is shown in the third graph. Note that the maxima of the field $E(x)$ are shifted by 90° with respect to those of the charge density distribution $\rho(x)$. The reason for this behavior is that the Maxwell equation $\nabla \cdot \mathbf{D} = \rho$ when applied to the present situation implies that $dE/dx = \rho/\epsilon$, and the spatial derivative that appears in this equation leads to a 90-degree phase shift between $E(x)$ and $\rho(x)$. The last graph in the figure shows the refractive index variation $\Delta n(x)$ that is produced through the linear electrooptic effect (Pockels effect) by the field $E(x)$.† Note that $\Delta n(x)$ is shifted by 90° with respect to the intensity distribution $I(x)$ that produces it. This phase shift has the important consequence that it can lead to the transfer of energy between the two incident beams. This transfer of energy is described in Section 11.6.

The properties of some photorefractive crystals are summarized in Table 11.4.1.

---

* Within the context of this book, we use the term *photorefractive effect* in the specific sense described in this section. Many workers in the field of nonlinear optics follow this convention. It should be noted that within certain communities, the term *photorefractive effect* is used to describe any light-induced change in refractive index.

† In drawing the figure, we have assumed that the electrooptic coefficient is positive. Note that the relation $\Delta(1/n^2) = r_{\text{eff}} E$ implies that $\Delta n = -\frac{1}{2} n^3 r_{\text{eff}} E$.

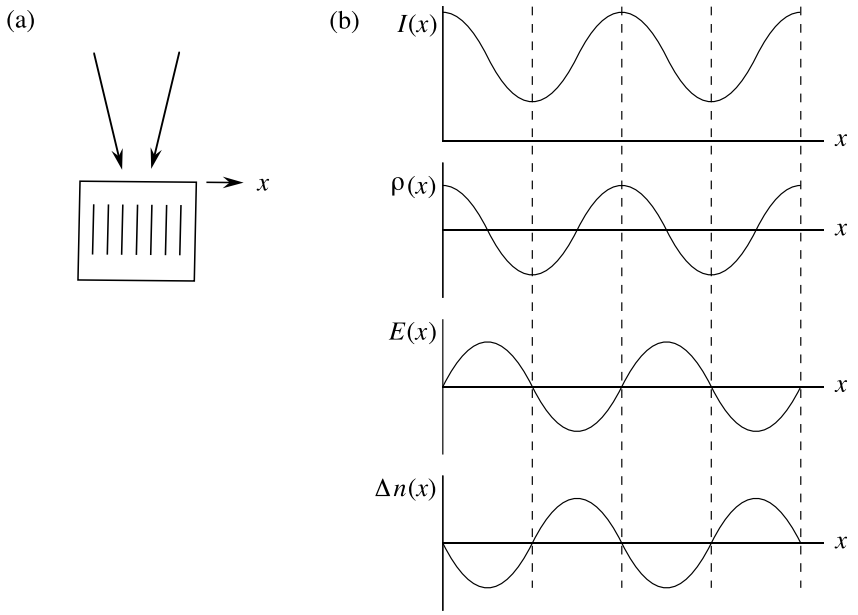

FIGURE 11.4.1: Origin of the photorefractive effect. (a) Two light beams form an interference pattern within a photorefractive crystal. (b) The resulting distributions of intensity $I(x)$, charge density $\rho(x)$, induced static field amplitude $E(x)$, and induced refractive index change $\Delta n(x)$ are illustrated.

TABLE 11.4.1: Properties of some photorefractive crystals[a].

Material	Useful wavelength range (μm)	Carrier drift length $\mu\tau E$ at $E = 2$ kV/cm (μm)	τ_d (sec)	$n^3 r_{\text{eff}}$ (pm/V)	$n^3 r_{\text{eff}}/\epsilon_{dc}$ (pm/V)
InP:Fe	0.85–1.3	3	10^{-4}	52	4.1
GaAs:Cr	0.8–1.8	3	10^{-4}	43	3.3
$LiNbO_3$:Fe^{3+}	0.4–0.7	$<10^{-4}$	300	320	11
$Bi_{12}SiO_{20}$	0.4–0.7	3	10^5	82	1.8
$Sr_{0.4}Ba_{0.6}Nb_2O_6$	0.4–0.6	–	10^2	2460	4.0
$BaTiO_3$	0.4–0.9	0.1	10^2	11,300	4.9
$KNbBO_3$	0.4–0.7	0.3	10^{-3}	690	14

[a] τ is the carrier recombination time; τ_d is the dielectric relaxation time in the dark. Adapted from Glass et al. (1984).

11.5 Photorefractive Equations of Kukhtarev et al.

In this section we see how to describe the photorefractive effect by means of a model (Fig. 11.5.1) due to Kukhtarev and co-workers.* This model presupposes that the photore-

* See Kukhtarev et al. (1977, 1979). This model is also described in several of the chapters of the book edited by Günter and Huignard (1988).

fractive effect is due solely to one type of charge carrier, which for definiteness we assume to be the electron. As illustrated in part (a) of the figure, we assume that the crystal contains N_A acceptors and N_D^0 donors per unit volume, with $N_A \ll N_D^0$. We assume that the acceptor levels are completely filled with electrons that have fallen from the donor levels and that these filled acceptor levels cannot be ionized by thermal or optical effects. Thus, at temperature $T = 0$ and in the absence of an optical field, each unit volume of the crystal contains N_A ionized donors, N_A electrons bound to acceptor impurities, and $N_D^0 - N_A$ neutral donor levels that can participate in the photorefractive effect. We further assume that electrons can be excited thermally or optically from the donor levels into the conduction band, as illustrated in part (b) of the figure. We let n_e, N_D^+, and N_D denote the number densities of conduction band electrons, ionized donors, and un-ionized donors, respectively. Note that $N_D + N_D^+$ must equal N_D^0, but that N_D^+ is not necessarily equal to n_e, because some donors lose their electrons to the acceptors and because electrons can migrate within the crystal, leading to regions that are not electrically neutral.

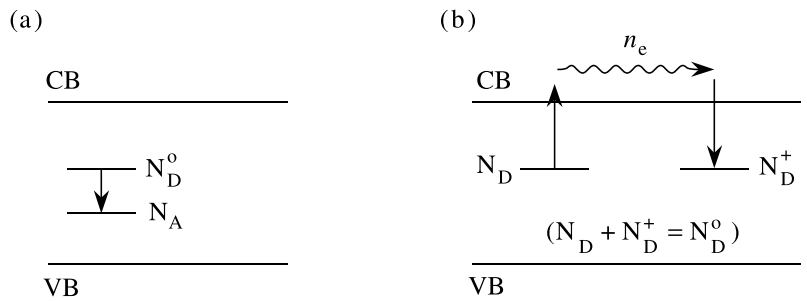

FIGURE 11.5.1: Energy levels and populations used in the model of Kukhtarev et al. to describe the photorefractive effect.

We next assume that the variation in level populations can be described by the rate equations

$$\frac{\partial N_D^+}{\partial t} = (sI + \beta)\left(N_D^0 - N_D^+\right) - \gamma n_e N_D^+, \tag{11.5.1}$$

$$\frac{\partial n_e}{\partial t} = \frac{\partial N_D^+}{\partial t} + \frac{1}{e}(\nabla \cdot \mathbf{j}) \tag{11.5.2}$$

where s is a constant proportional to the photoionization cross section of a donor, β is the thermal generation rate, γ is the recombination coefficient, $-e$ is the charge of the electron, and $\mathbf{j}$ is the electrical current density. Eq. (11.5.1) states that the ionized donor concentration can increase by thermal ionization or photoionization of unionized donors and can decrease by recombination. Eq. (11.5.2) states that the mobile electron concentration can increase in any

small region either because of the ionization of donor atoms or because of the flow of electrons into the local region. The flow of current is described by the equation

$$\mathbf{j} = n_e e\mu \mathbf{E} + eD\nabla n_e + \mathbf{j}_{\text{ph}}, \tag{11.5.3}$$

where μ is the electron mobility, D is the diffusion constant (which by the Einstein relation is equal to $k_B T\mu/e$), and $\mathbf{j}_{\text{ph}}$ is the photovoltaic (also known as the photogalvanic) contribution to the current. The last contribution results from the tendency of the photoionization process to eject the electron in a preferred direction in anisotropic crystals. For some materials (such as barium titanate and bismuth silicon oxide) this contribution to $\mathbf{j}$ is negligible, although for others (such as lithium niobate) it is very important. For lithium niobate $\mathbf{j}_{\text{ph}}$ has the form $\mathbf{j}_{\text{ph}} = pI\hat{\mathbf{c}}$, where $\hat{\mathbf{c}}$ is a unit vector in the direction of the optic axis of the crystal and p is a constant. The importance of the photovoltaic current has been discussed by Glass (1978) and Glass et al. (1974).

The field $\mathbf{E}$ appearing in Eq. (11.5.3) is the static (or possibly low-frequency) electric field appearing within the crystal due to any applied voltage or to any charge separation within the crystal. It must satisfy the Maxwell equation

$$\epsilon_{dc}\nabla \cdot \mathbf{E} = -e\left(n_e + N_A - N_D^+\right), \tag{11.5.4}$$

where ϵ_{dc} is the static dielectric constant of the crystal. The modification of the optical properties is described by assuming that the optical-frequency dielectric constant is changed by an amount

$$\Delta\epsilon = -\epsilon^2 r_{\text{eff}}|E|. \tag{11.5.5}$$

For simplicity, here we are treating the dielectric properties in the scalar approximation; the tensor properties can be treated explicitly using the formalism developed in Section 11.2.* Note that the scalar form of Eq. (11.2.13a) is $\Delta(1/\epsilon) = r_{\text{eff}}|\mathbf{E}|$, from which Eq. (11.5.5) follows directly. The optical field $\tilde{E}_{\text{opt}}$ is assumed to obey the wave equation

$$\nabla^2 \tilde{E}_{\text{opt}} + \frac{1}{c^2}\frac{\partial^2}{\partial t^2}(\epsilon + \Delta\epsilon)\tilde{E}_{\text{opt}} = 0. \tag{11.5.6}$$

Eqs. (11.5.1) through (11.5.6) constitute the photorefractive equations of Kukhtarev et al. They have been solved in a variety of special cases and have been found to provide an adequate description of most photorefractive phenomena. We shall consider their solution in special cases in the next two sections.

* See also the calculation of r_{eff} for one particular case in Eq. (11.6.14b) in the next section.

11.6 Two-Beam Coupling in Photorefractive Materials

Under certain circumstances, two beams of light can interact in a photorefractive crystal in such a manner that energy is transferred from one beam to the other. This process, which is often known as two-beam coupling, can be used, for example, to amplify a weak, image-bearing signal beam by means of an intense pump beam. Exponential gains of 10 per centimeter are routinely observed.

A typical geometry for studying two-beam coupling is shown in Fig. 11.6.1. Signal and pump waves, of amplitudes A_s and A_p, respectively, interfere to form a nonuniform intensity distribution within the crystal. Because of the nonlinear response of the crystal, this nonuniform intensity distribution produces a refractive index grating within the material. However, this grating is displaced from the intensity distribution in the direction of the positive (or negative, depending on the sign of the dominant charge carrier and the sign of the effective electrooptic coefficient) crystalline c axis. As a result of this phase shift, the light scattered from A_p and A_s interferes constructively with A_s, whereas the light scattered from A_s into A_p interferes destructively with A_p, and consequently the signal wave is amplified whereas the pump wave is attenuated.

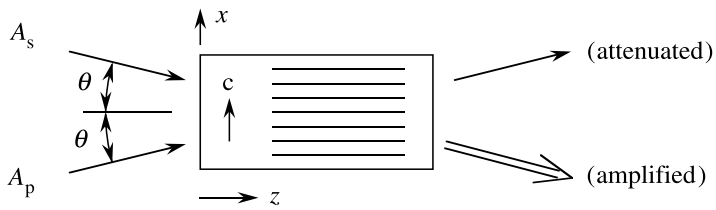

FIGURE 11.6.1: Typical geometry for studying two-beam coupling in a photorefractive crystal.

In order to describe this process mathematically, we assume that the optical field within the crystal can be represented as

$$\tilde{E}_{\text{opt}}(\mathbf{r}, t) = \left[A_p(z)e^{i\mathbf{k_p}\cdot\mathbf{r}} + A_s(z)e^{i\mathbf{k_s}\cdot\mathbf{r}}\right]e^{-i\omega t} + \text{c.c.} \tag{11.6.1}$$

We assume that $A_p(z)$ and $A_s(z)$ are slowly varying functions of the coordinate z. The intensity distribution of the light within the crystal can be expressed as $I = n_0\epsilon_0 c\langle\tilde{E}^2_{\text{opt}}\rangle$ or as

$$I = I_0 + \left(I_1 e^{iqx} + \text{c.c.}\right), \tag{11.6.2a}$$

where

$$\begin{aligned} I_0 &= 2n_0\epsilon_0 c\left(|A_p|^2 + |A_s|^2\right), \\ I_1 &= 2n_0\epsilon_0 c\left(A_p A_s^*\right)(\hat{\mathbf{e}}_\mathbf{p}\cdot\hat{\mathbf{e}}_\mathbf{s}), \quad \text{and} \quad \mathbf{q} \equiv q\hat{\mathbf{x}} = \mathbf{k_p} - \mathbf{k_s}. \end{aligned} \tag{11.6.2b}$$

Here $\hat{e}_p$ and $\hat{e}_s$ are the polarization unit vectors of the pump and signal waves, which are assumed to be linearly polarized. The quantity $\mathbf{q}$ is known as the grating wavevector. Note that the intensity distribution can also be described by the expression

$$I = I_0\big[1 + m\cos(qx + \phi)\big], \tag{11.6.3}$$

where $m = 2|I_1|/I_0$ is known as the modulation index and where $\phi = \tan^{-1}(\operatorname{Im} I_1/\operatorname{Re} I_1)$.

In order to determine how the optical properties of the photorefractive material are modified by the presence of the pump and signal fields, we first solve Eqs. (11.5.1) through (11.5.4) of Kukhtarev et al. to find the static electric field $\mathbf{E}$ induced by the intensity distribution of Eqs. (11.6.2). This static electric field can then be used to calculate the change in the optical-frequency dielectric constant through use of Eq. (11.5.5). Since Eqs. (11.5.1) through (11.5.4) are nonlinear (i.e., they contain products of the unknown quantities n_e, N_D^+, $\mathbf{j}$, and $\mathbf{E}$), they cannot easily be solved exactly. For this reason, we assume that the depth of modulation m is small (i.e., $|I_1| \ll I_0$) and seek an approximate steady-state solution of Eqs. (11.5.1) through (11.5.4) in the form

$$\begin{aligned} E &= E_0 + \big(E_1 e^{iqx} + \text{c.c.}\big), & j &= j_0 + \big(j_1 e^{iqx} + \text{c.c.}\big), \\ n_e &= n_{e0} + \big(n_{e1} e^{iqx} + \text{c.c.}\big), & N_D^+ &= N_{D0}^+ + \big(N_{D1}^+ d^{iqx} + \text{c.c.}\big), \end{aligned} \tag{11.6.4}$$

where $E = E\hat{\mathbf{x}}$ and $\mathbf{j} = j\hat{\mathbf{x}}$. We assume that the quantities E_1, j_1, n_{e1}, and N_{D1} are small in the sense that the product of any two of them can be neglected.

We next introduce Eq. (11.6.4) into Eqs. (11.5.1) through (11.5.4) and equate terms with common x dependences. We thereby find several sets of equations. The set that is independent of the x coordinate depends only on the large quantities (subscript zero) and is given (in the same order as Eqs. (11.5.1) through (11.5.4)) by

$$(sI_0 + \beta)\big(N_D^0 - N_{D0}^+\big) = \gamma n_{e0} N_{D0}^+, \tag{11.6.5a}$$

$$j_0 = \text{constant}, \tag{11.6.5b}$$

$$j_0 = n_{e0} e\mu E_0 + j_{\text{ph},0}, \tag{11.6.5c}$$

$$N_{D0}^+ = n_{e0} + N_A. \tag{11.6.5d}$$

Eqs. (11.6.5a) and (11.6.5d) can be solved directly to determine the mean electron density n_{e0} and mean ionized donor density N_{D0}^+. Since in most realistic cases the inequality $n_{e0} \ll N_A$ is satisfied, the densities are given simply by

$$N_{D0}^+ = N_A, \tag{11.6.6a}$$

$$n_{e0} = \frac{(sI_0 + \beta)\big(N_D^0 - N_A\big)}{\gamma N_A}. \tag{11.6.6b}$$

The two remaining equations, (11.6.5b) and (11.6.5c), determine the mean current density j_0 and mean field E_0. Let us assume for simplicity that the photovoltaic contribution j_{ph} is negligible for the material under consideration. The value of E_0 then depends on the properties of any external electric circuit to which the crystal is connected. In the common situation in which no voltage is externally applied to the crystal, E_0 and hence j_0 vanish.

We next consider the equation for the first-order quantities (quantities with the subscript 1) by considering the portions of Eqs. (11.5.1) through (11.5.4) with the spatial dependence e^{iqx}. The resulting equations are (we assume that $E_0 = 0$):

$$sI_1\left(N_D^0 - N_A\right) - (sI_0 + \beta)N_{D1}^+ = \gamma n_{e0} N_{D1}^+ + \gamma n_{e1} N_A, \tag{11.6.7a}$$

$$j_1 = 0, \tag{11.6.7b}$$

$$-n_{e0} e E_1 = iqk_B T n_{e1}, \tag{11.6.7c}$$

$$iq\epsilon_0 \epsilon_{dc} E_1 = -e\left(n_{e1} - N_{D1}^+\right). \tag{11.6.7d}$$

We solve these equations algebraically (again assuming that $n_{e0} \ll N_A$) to find that the amplitude of the spatially varying part of the static electric field is given by

$$E_1 = -i\left(\frac{sI_1}{sI_0 + \beta}\right)\left(\frac{E_D}{1 + E_D/E_q}\right), \tag{11.6.8}$$

where we have introduced the characteristic field strengths

$$E_D = \frac{qk_B T}{e}, \qquad E_q = \frac{e}{\epsilon_0 \epsilon_{\text{de}} q} N_{\text{eff}}, \tag{11.6.9}$$

where $N_{\text{eff}} = N_A(N_D^0 - N_A)/N_D^0$ can be interpreted as an effective trap density. Note that in the common circumstance where $N_A \ll N_D^0$, N_{eff} is given approximately by $N_{\text{eff}} \simeq N_A$. The quantity E_D is called the diffusion field strength and is a measure of the field strength required to inhibit the separation of charge due to thermal agitation. The quantity E_q is called the maximum space charge field and is a measure of the maximum electric field that can be created by redistributing charge of mean density eN_{eff} over the characteristic distance $2\pi/q$. Note from Eq. (11.6.8) that E_1 is shifted in phase with respect to the intensity distribution I_1 and that E_1 is proportional to the depth of modulation m in the common case of $\beta \ll sI_0$.

Recall that the change in the optical-frequency dielectric constant is proportional to the amplitude E_1 of the spatially modulated component of the static electric field. For this reason, it is often of practical interest to maximize the value of E_1. We see from Eq. (11.6.8) that E_1 is proportional to the product of the factor $sI_1/(sI_0 + \beta)$, which can be maximized by increasing the depth of modulation $m = 2|I_1|/I_0$,* with the factor $E_D/(1 + E_D/E_q)$. Since each of the characteristic field strengths E_D and E_q depends on the grating wavevector, this second factor

* Recall, however, that the present derivation is valid only if $m \ll 1$.

can be maximized by using the optimum value of q. To show the dependence of E_1 on q, we can rewrite Eq. (11.6.8) as

$$E_1 = -i\left(\frac{sI_1}{sI_0+\beta}\right)E_{\text{opt}}\frac{2(q/q_{\text{opt}})}{1+(q/q_{\text{opt}})^2}, \tag{11.6.10a}$$

where

$$q_{\text{opt}} = \left(\frac{N_{\text{eff}}e^2}{k_BT\epsilon_0\epsilon_{\text{dc}}}\right)^{1/2}, \qquad E_{\text{opt}} = \left(\frac{N_{\text{eff}}k_BT}{4\epsilon_0\epsilon_{\text{dc}}}\right)^{1/2}. \tag{11.6.10b}$$

Note that q_{opt} is of the order of magnitude of the Debye–Hückel screening wave number of Eq. (4.6.7).

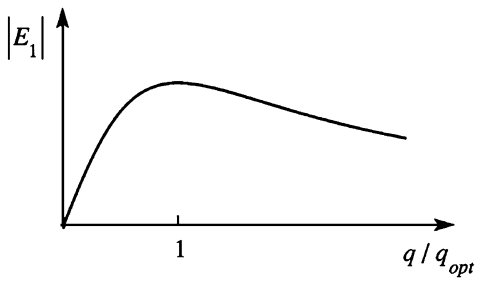

FIGURE 11.6.2: Dependence of the modulated component of the space charge field on the magnitude q of the grating wavevector.

The dependence of E_1 on q is shown in Fig. 11.6.2. Note that the grating wavevector q can be varied experimentally by controlling the angle between the pump and signal beams, since (see Fig. 11.6.1) q is given by the formula

$$q = 2n\frac{\omega}{c}\sin\theta. \tag{11.6.11}$$

Through an experimental determination of the optimum value of the magnitude of the grating wavevector, the value of the effective trap density N_{eff} can be obtained through use of Eq. (11.6.10b).

Let us next calculate the spatial growth rate that the signal wave experiences as the result of two-beam coupling in photorefractive materials. For simplicity, we assume that the photoionization rate sI_0 is much greater than the thermal ionization rate β (which is the usual case in practice), so the field amplitude E_1 of Eq. (11.6.8) can be expressed through use of Eqs. (11.6.2) as

$$E_1 = -i\frac{A_pA_s^*}{|A_s|^2+|A_p|^2}(\hat{e}_p\cdot\hat{e}_s)E_m, \tag{11.6.12a}$$

where

$$E_m = \frac{E_D}{1 + E_D/E_q}. \tag{11.6.12b}$$

According to Eq. (11.5.5), this field produces a change in the dielectric constant of amplitude $\Delta\epsilon = -\epsilon^2 r_{\text{eff}} E_1$. For the particular geometry of Fig. 11.6.1, the product $\epsilon^2 r_{\text{eff}}$ has the form (Feinberg et al., 1980; see also Feinberg and MacDonald, 1989)

$$\epsilon^2 r_{\text{eff}} = \sum_{ijklm} r_{ijk} \left(\epsilon_{il} \hat{e}_l^s\right)\left(\epsilon_{jm} \hat{e}_m^p\right) \hat{q}_k, \tag{11.6.13}$$

where $\hat{e}_l^s$ and $\hat{e}_m^p$ denote the l and m cartesian components of the polarization unit vectors of the signal and pump waves, respectively, and $\hat{q}_k$ denotes the k cartesian component of a unit vector in the direction of the grating vector. For crystals of point group $4mm$ (such as barium titanate), one finds that for ordinary waves

$$r_{\text{eff}} = r_{13} \sin\left(\frac{\alpha_s + \alpha_p}{2}\right) \tag{11.6.14a}$$

and that for extraordinary waves

$$\begin{aligned} r_{\text{eff}} = n^{-4}\big[&n_0^4 r_{13} \cos\alpha_s \cos\alpha_p + 2n_e^2 n_0^2 r_{42} \cos\tfrac{1}{2}(\alpha_s + \alpha_p) \\ &+ n_e^4 r_{33} \sin\alpha_s \sin\alpha_p\big] \sin\tfrac{1}{2}(\alpha_s + \alpha_p). \end{aligned} \tag{11.6.14b}$$

Here α_s and α_p denote the angles between the propagation vectors of the signal and pump waves and the positive crystalline c axis, respectively, and n is the refractive index experienced by the beam that scatters off the grating.

Note from Table 11.2.1 that for barium titanate the electrooptic coefficient r_{42} is much larger than either r_{13} or r_{33}. We see from Eqs. (11.6.14) that only through the use of light of extraordinary polarization can one utilize this large component of the electrooptic tensor.

The change in the dielectric constant $\Delta\epsilon = -\epsilon^2 r_{\text{eff}} E_1$ produces a nonlinear polarization given by

$$P^{\text{NL}} = \left(\Delta\epsilon\, e^{i\mathbf{q}\cdot\mathbf{r}} + \text{c.c.}\right)\left(A_s e^{i\mathbf{k_s}\cdot\mathbf{r}} + A_p e^{i\mathbf{k_p}\cdot\mathbf{r}}\right). \tag{11.6.15}$$

Recall that $\mathbf{q} = \mathbf{k_p} - \mathbf{k_s}$. The part of the nonlinear polarization having the spatial variation $\exp(i\mathbf{k_s}\cdot\mathbf{r})$ can act as a phase-matched source term for the signal wave and is given by

$$P_s^{\text{NL}} = \Delta\epsilon^* A_p e^{i\mathbf{k_s}\cdot\mathbf{r}} = -i\epsilon^2 r_{\text{eff}} E_m \frac{|A_p|^2 A_s}{|A_p|^2 + |A_s|^2} e^{i\mathbf{k_s}\cdot\mathbf{r}}. \tag{11.6.16a}$$

Likewise, the portion of P^{NL} that can act as a phase-matched source term for the pump wave is given by

$$P_p^{\mathrm{NL}} = \Delta\epsilon A_s e^{i\mathbf{k_p}\cdot\mathbf{r}} = i\epsilon^2 r_{\mathrm{eff}} E_m \frac{|A_s|^2 A_p}{|A_p|^2 + |A_s|^2} e^{i\mathbf{k_p}\cdot\mathbf{r}}. \tag{11.6.16b}$$

We next derive coupled-amplitude equations for the pump and signal fields using the formalism described in Section 2.1. We define z_s and z_p to be distances measured along the signal and pump propagation directions. We find that in the slowly varying amplitude approximation the signal amplitude varies as

$$2ik\frac{dA_s}{dz_s} e^{i\mathbf{k_s}\cdot\mathbf{r}} = -\frac{\omega^2}{c^2} P_s^{\mathrm{NL}}, \tag{11.6.17a}$$

which through use of Eq. (11.6.16a) becomes

$$\frac{dA_s}{dz_s} = \frac{\omega}{2c} n^3 r_{\mathrm{eff}} E_m \frac{|A_p|^2 A_s}{|A_p|^2 + |A_s|^2}. \tag{11.6.17b}$$

We find that the intensity $I_s = 2n\epsilon_0 c|A_s|^2$ of the signal wave varies spatially as $dI_s/dz_s = n\epsilon_0 c(A_s^* dA_s/dz_s + \text{c.c.})$, or as

$$\frac{dI_s}{dz_s} = \Gamma \frac{I_s I_p}{I_s + I_p}, \tag{11.6.18a}$$

where*

$$\Gamma = \frac{\omega}{c} n^3 r_{\mathrm{eff}} E_m. \tag{11.6.18b}$$

A similar derivation shows that the pump intensity varies spatially as

$$\frac{dI_p}{dz_p} = -\Gamma \frac{I_s I_p}{I_s + I_p}. \tag{11.6.18c}$$

Note that Eq. (11.6.18a) predicts that the signal intensity grows exponentially with propagation distance in the common limit $I_s \ll I_p$.† The strong amplification available from photorefractive two-beam coupling allows this process to be used for various practical applications. For

* Following convention, we use the same symbol Γ to denote the photorefractive gain coefficient and the retardation of Section 11.3.

† Here we implicitly assume that Γ is a positive quantity. If Γ is negative, the wave that we have been calling the pump wave will be amplified and the wave that we have been calling the signal wave will be attenuated. The sign of Γ depends on the sign of r_{eff}, which can be either positive or negative, and on the sign of E_m. Note that, according to Eqs. (11.6.9) and (11.6.12b), the sign of E_m depends on the sign of the dominant charge carrier (our derivation has assumed the case of an electron) and on the sign of q, which is the x component of $\mathbf{k_p} - \mathbf{k_s}$. For the case of barium titanate, the dominant charge carriers are usually holes, and the wave whose wavevector has a positive component along the crystalline c axis is amplified.

the application of photorefractive two-beam coupling to the design of efficient polarizers, see Heebner et al. (2000).

The treatment of two-beam coupling given above has assumed that the system is in steady state. Two-beam coupling under transient conditions can also be treated using the material equations of Kukhtarev et al. It has been shown (Kukhtarev et al., 1977; Refrégier et al., 1985; Valley, 1987) that, under the assumption that $n_e \ll N_D^+$, $N_D^+ \ll N_D^0$, and $\beta \ll sI_0$, the electric field amplitude E_1 obeys the equation

$$\tau \frac{\partial E_1}{\partial t} + E_1 = -iE_m \frac{A_p A_s^*}{|A_p|^2 + |A_s|^2} (\hat{e}_p \cdot \hat{e}_s) \tag{11.6.19}$$

with E_m given by Eq. (11.6.12b) and with the response time τ given by

$$\tau = \tau_d \frac{1 + E_D/E_M}{1 + E_D/E_q}, \tag{11.6.20a}$$

where

$$\tau_d = \frac{\epsilon_0 \epsilon_{dc}}{e\mu n_{e0}}, \qquad E_M = \frac{\gamma N_A}{q\mu}. \tag{11.6.20b}$$

Here, as in Section 11.5, γ denotes the recombination coefficient and μ denotes the carrier mobility. Note that the photorefractive response time τ scales linearly with the dielectric relaxation time τ_d.* Since the mean electron density n_{e0} increases linearly with optical intensity (see Eq. (11.6.6b)), we see that the photorefractive response time becomes faster when the crystal is excited using high optical intensities.

We next write the coupled-amplitude equations for the pump and signal fields in terms of the field amplitude E_1 as

$$\frac{\partial A_p}{\partial x_p} = \frac{-\omega}{2n_p c} r_{\text{eff}} A_s E_1, \tag{11.6.21a}$$

$$\frac{\partial A_s}{\partial x_s} = \frac{-\omega}{2n_s c} r_{\text{eff}} A_p E_1. \tag{11.6.21b}$$

Eqs. (11.6.19) through (11.6.21) describe the transient behavior of two-beam coupling.

* The dielectric relaxation time is the characteristic time in which charge imbalances neutralize in a conducting material. The expression for the dielectric relaxation time is derived by combining the equation of continuity $\partial\rho/\partial t = -\nabla \cdot \mathbf{j}$ with Ohm's law in the form $\mathbf{j} = \sigma\mathbf{E}$ to find that $\partial\rho/\partial t = -\sigma\nabla \cdot \mathbf{E} = -(\sigma/\epsilon_0\epsilon_{dc})\nabla \cdot \mathbf{D} = -(\sigma/\epsilon_0\epsilon_{dc})\rho \equiv -\rho/\tau_d$. By equating the electrical conductivity σ with the product $n_{e0}e\mu$, where μ is the carrier mobility, we obtain the expression for τ_d quoted in the text.

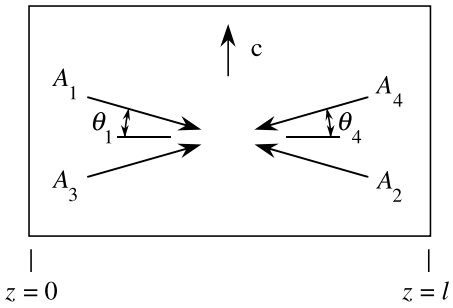

FIGURE 11.7.1: Geometry of four-wave mixing in a photorefractive material.

11.7 Four-Wave Mixing in Photorefractive Materials

Next we consider the mutual interaction of four beams of light in a photorefractive crystal. We assume the geometry of Fig. 11.7.1. Note that the pump beams 1 and 2 are counterpropagating, as are beams 3 and 4. Thus the interaction shown in the figure can be used to generate beam 4 as the phase conjugate of beam 3.

The general problem of the interaction of four beams of light in a photorefractive material is very complicated, because the material response consists of four distinct gratings—namely, one grating due to the interference of beams 1 and 3 and of 2 and 4, one grating due to the interference of beams 1 and 4 and of 2 and 3, one grating due to the inference of beams 1 and 2, and one grating due to the interference of beams 3 and 4. However, under certain experimental situations, only one of these gratings leads to appreciable nonlinear coupling among the beams. If one assumes that the polarizations, propagation directions, and coherence properties of the input beams are selected so that only the grating due to the interference of beams 1 and 3 and beams 2 and 4 is important, the coupled-amplitude equations describing the propagation of the four beams become (Cronin-Golomb et al., 1984; see also Fischer et al., 1981)

$$\frac{dA_1}{dz} = -\frac{\gamma}{S_0}\left(A_1 A_3^* + A_2^* A_4\right) A_3 - \alpha A_1, \tag{11.7.1a}$$

$$\frac{dA_2}{dz} = -\frac{\gamma}{S_0}\left(A_1^* A_3 + A_2 A_4^*\right) A_4 + \alpha A_2, \tag{11.7.1b}$$

$$\frac{dA_3}{dz} = \frac{\gamma}{S_0}\left(A_1^* A_3 + A_2 A_4^*\right) A_1 - \alpha A_3, \tag{11.7.1c}$$

$$\frac{dA_4}{dz} = \frac{\gamma}{S_0}\left(A_1 A_3^* + A_2^* A_4\right) A_2 + \alpha A_4. \tag{11.7.1d}$$

In these equations, we have introduced the following quantities:

$$\gamma = \frac{\omega r_{\text{eff}} n_0^3 E_m}{2c \cos\theta} \tag{11.7.2a}$$

with E_m given by Eq. (11.6.12b),

$$S_0 = \sum_{i=1}^{4} |A_i|^2, \tag{11.7.2b}$$

and $\alpha = \frac{1}{2}\alpha_0/\cos\theta$, where α_0 is the intensity absorption coefficient of the material and where for simplicity we have assumed that $\theta = \theta_1 = \theta_4$.

Cronin-Golomb et al. (1984) have shown that Eqs. (11.7.1) can be solved for a large number of cases of interest. The solutions show a variety of interesting features, including amplified reflection, self-oscillation, and bistability.

11.7.1 Externally Self-Pumped Phase-Conjugate Mirror

One interesting feature of four-wave mixing in photorefractive materials is that it can be used to construct a self-pumped phase-conjugate mirror of the sort illustrated in Fig. 11.7.2. In such a device, only the signal wave A_3 is applied externally. Waves A_1 and A_2 grow from noise within the resonator that surrounds the photorefractive crystal. Oscillation occurs because wave A_1 is amplified at the expense of wave A_3 by the process of two-beam coupling. The output wave A_4 is generated by four-wave mixing involving waves A_1, A_2, and A_3. Such a device was constructed by White et al. (1982) and is described further by Cronin-Golomb et al. (1984).

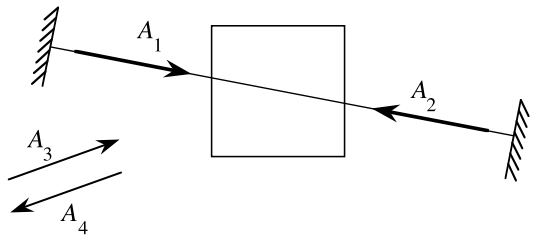

FIGURE 11.7.2: Geometry of the externally self-pumped phase-conjugate mirror. Only the A_3 wave is applied externally; this wave excites the oscillation of the waves A_1 and A_2, which act as pump waves for the four-wave mixing process that generates the conjugate wave A_4.

11.7.2 Internally Self-Pumped Phase-Conjugate Mirror

Even more remarkable than the device just described is the internally self-pumped phase conjugate mirror, which is illustrated in Fig. 11.7.3. Once again, only the signal wave A_3 is applied externally. By means of a complicated nonlinear process analogous to self-focusing, beams A_1 and A_2 are created. Reflection of these waves at the corner of the crystal feeds these waves back into the path of the applied wave A_3. Four-wave mixing processes involving waves A_1,

A_2, and A_3 then create the output wave A_4 as the phase conjugate of A_3. This device was first demonstrated by Feinberg (1982) and analyzed theoretically by MacDonald and Feinberg (1983). Because of the complicated nature of the coupling that occurs in this device, it can produce complicated dynamical behavior including deterministic chaos, as demonstrated by Gauthier et al. (1987). Because of the ease with which a phase-conjugate signal can be produced, such devices lend themselves to practical applications such as the construction of new types of interferometers (Gauthier et al., 1989).

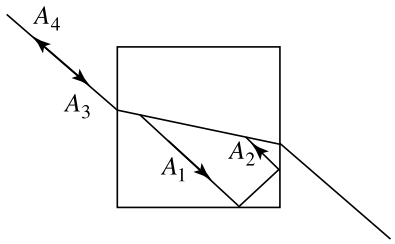

FIGURE 11.7.3: Geometry of the internally self-pumped phase conjugate mirror. Only the A_3 wave is applied externally; this wave excites the oscillation of the waves A_1 and A_2, which act as pump waves for the four-wave mixing process that generates the conjugate wave A_4.

11.7.3 Double Phase-Conjugate Mirror

Another application of four-wave mixing in photorefractive crystals is the double phase-conjugate mirror of Fig. 11.7.4. In such a device the waves A_2 and A_3 are applied externally; these waves are assumed to be mutually incoherent, so that no gratings are formed by their interference. The nonlinear interaction leads to the generation of the output wave A_1, which is the phase conjugate of A_2, and to the output wave A_4, which is the phase conjugate of A_3. However, A_1 is phase-coherent with A_3, whereas A_4 is phase-coherent with A_2. The double phase-conjugate mirror possesses the remarkable property that one of the output waves can be an amplified phase-conjugate wave, even though the two input waves are mutually incoherent.

The nature of the nonlinear coupling that produces the double phase-conjugate mirror can be understood from the coupled-amplitude equations (11.7.1). For simplicity, we consider the limit in which α is negligible and in which the input waves A_2 and A_3 are not modified by the nonlinear interaction, so that only Eqs. (11.7.1a) and (11.7.1d) need to be considered. We see that each output wave is driven by two terms, one of which is a two-beam-coupling term that tends to amplify the output wave, and the other of which is a four-wave-mixing term that causes each output to be the phase conjugate of its input wave. It has been shown by Cronin-Golomb et al. (1984) and by Weiss et al. (1987) that the requirement for the generation of the two output waves is that $|\gamma|l$ be greater than 2. Operation of the double phase-conjugate mirror has been demonstrated experimentally by Weiss et al. (1987).

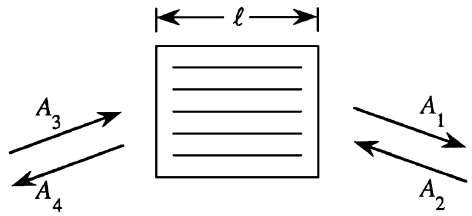

FIGURE 11.7.4: Geometry of the double phase-conjugate mirror. Waves A_2 and A_3 are applied externally and need not be phase-coherent. The generated wave A_1 is the phase conjugate of A_2, and the generated wave A_4 is the phase conjugate of A_3.

11.7.4 Other Applications of Photorefractive Nonlinear Optics

Because the photorefractive effect leads to a large nonlinear response, it lends itself to a variety of applications. Certain of these have applications have been reviewed by Günter and Huignard (1988, 1989) and by Boyd and Grynberg (1992). The use of the photorefractive effect to support spatial solitons has been reviewed by Królikowski et al. (2003).

Problems

1. *Numerical evaluation of photorefractive quantities.* Consider the process of two-beam coupling in barium titanate in the geometry of Fig. 11.6.1. Estimate the numerical values of the physical quantities E_D, E_q, E_{opt}, E_1, r_{eff}, $\Delta\epsilon$, and Γ. Assume that the effective trap density N_{eff} is equal to 10^{12} cm^{-3}, that the thermal generation rate is negligible, that the modulation index m is 10^{-3}, and that $\theta_s = \theta_p = 5°$.
2. *Transient two-beam coupling.* Verify Eq. (11.6.19).
3. *Relation between electrooptic and nonlinear optics tensors.* Determine the mathematical relationship between the second-order susceptibility $\chi^{(2)}_{ijk}$ and the linear electrooptic coefficient r_{ijk}. Similarly, determine the mathematical relationship between the third-order susceptibility $\chi^{(3)}_{ijkl}$ and the quadratic electrooptic coefficient s_{ijkl}.

References

Electrooptic Effect

Born, M., Wolf, E., 1975. Principles of Optics. Pergamon, London.

Cook Jr., W.R., Jaffe, J., 1979. Electrooptic Coefficients. In: Hellwege, K.-H. (Ed.), Landolt-Bornstein, New Series, vol. II. Springer-Verlag, Berlin, pp. 552–651.

Kaminow, I.P., 1974. An Introduction to Electrooptic Devices. Academic Press, New York.

Thompson, B.J., Hartfield, E., 1978. In: Driscoll, W.G., Vaughan, W. (Eds.), Handbook of Optics. McGraw-Hill, New York.

Yariv, A., Yeh, P., 1984. Optical Waves in Crystals. Wiley, New York.

Photorefractive Effect

Boyd, R.W., Grynberg, G., 1992. Optical phase conjugation. In: Agrawal, G.P., Boyd, R.W. (Eds.), Contemporary Nonlinear Optics. Academic Press, Boston.
Cronin-Golomb, M., Fischer, B., White, J.O., Yariv, A., 1984. IEEE J. Quantum Electron. 20, 12.
Feinberg, J., 1982. Opt. Lett. 7, 486.
Feinberg, J., MacDonald, K.R., 1989. In: Günter, P., Huignard, J.-P. (Eds.), Photorefractive Materials and Their Applications, vol. II. Springer-Verlag, Berlin.
Feinberg, J., Heiman, D., Tanguay Jr., A.R., Hellwarth, R.W., 1980. J. Appl. Phys. 5, 1297.
Fischer, B., Cronin-Golomb, M., White, J.O., Yariv, A., 1981. Opt. Lett. 6, 519.
Gauthier, D.J., Narum, P., Boyd, R.W., 1987. Phys. Rev. Lett. 58, 16.
Gauthier, D.J., Boyd, R.W., Jungquist, R.K., Lisson, J.B., Voci, L.L., 1989. Opt. Lett. 14, 325.
Glass, A.M., 1978. Opt. Eng. 17, 470.
Glass, A.M., von der Linde, D., Negran, T.J., 1974. Appl. Phys. Lett. 25, 233.
Glass, A.M., Johnson, A.M., Olson, D.H., Simpson, W., Ballman, A.A., 1984. Appl. Phys. Lett. 44, 948.
Günter, P., Huignard, J.-P. (Eds.), 1988. Photorefractive Materials and Their Applications, Part I. Springer-Verlag, Berlin.
Günter, P., Huignard, J.-P. (Eds.), 1989. Photorefractive Materials and Their Applications, Part II. Springer-Verlag, Berlin.
Heebner, J.E., Bennink, R.S., Boyd, R.W., Fisher, R.A., 2000. Opt. Lett. 25, 257.
Królikowski, W., Luther-Davies, B., Denz, C., 2003. IEEE J. Quantum Electron. 39, 3.
Kukhtarev, N., Markov, V.B., Odulov, S.G., 1977. Opt. Commun. 23, 338.
Kukhtarev, N., Markov, V.B., Odulov, S.G., Soskin, M.S., Vinetskii, V.L., 1979. Ferroelectrics 22, 949–960, 961–964.
MacDonald, K.R., Feinberg, J., 1983. J. Opt. Soc. Am. 73, 548.
Refrégier, Ph., Solymar, L., Rabjenbach, H., Huignard, J.P., 1985. J. Appl. Phys. 58, 45.
Valley, G.C., 1987. J. Opt. Soc. Am. B 4 (14), 934.
Weiss, S., Sternklar, S., Fischer, B., 1987. Opt. Lett. 12, 114.
White, J.O., Cronin-Golomb, M., Fischer, B., Yariv, A., 1982. Appl. Phys. Lett. 40, 450.